General Disclaimer

One or more of the Following Statements may affect this Document

- This document has been reproduced from the best copy furnished by the organizational source. It is being released in the interest of making available as much information as possible.

- This document may contain data, which exceeds the sheet parameters. It was furnished in this condition by the organizational source and is the best copy available.

- This document may contain tone-on-tone or color graphs, charts and/or pictures, which have been reproduced in black and white.

- This document is paginated as submitted by the original source.

- Portions of this document are not fully legible due to the historical nature of some of the material. However, it is the best reproduction available from the original submission.

Polytechnic Institute of New York

AERODYNAMICS LABORATORIES
~
DEPARTMENT OF MECHANICAL and AEROSPACE ENGINEERING

AN OLD INTEGRATION SCHEME FOR COMPRESSIBLE FLOWS REVISITED, REFURBISHED AND PUT TO WORK

BY GINO MORETTI

September 1978

Grant No. NSG 1248

Grant No. DAAG 29-77-G-0072,
Project No. P14369-E

Contract No. N00014-75-C-0511,
Project No. NR 061-135

POLY M/AE Report No. 78-22

AN OLD INTEGRATION SCHEME FOR COMPRESSIBLE FLOWS REVISITED, REFURBISHED AND PUT TO WORK

BY

Gino Moretti

This research was conducted under the sponsorship of the NASA Langley Research Center under Grant No. NSG 1248, the Army Research Office under Grant No. DAAG 29-77-G-0072, Project No. P14369-E and by the Office of Naval Research under Contract No. N00014-75-C-0511, Project No. NR 061-135.

POLYTECHNIC INSTITUTE OF NEW YORK

Aerodynamics Laboratories

September 1978

POLY M/AE Report No. 78-22

AN OLD INTEGRATION SCHEME FOR COMPRESSIBLE FLOWS REVISITED, REFURBISHED AND PUT TO WORK*

by

Gino Moretti**

Polytechnic Institute of New York
Aerodynamics Laboratories
Farmingdale, New York

ABSTRACT

A scheme for integrating the Euler equations of compressible flow in any hyperbolic case is presented. The scheme relies on the concept of characteristics but is strictly a finite difference scheme. Improvements in accuracy and physical consistence due to the scheme are discussed and results of its application to complex flows are shown.

* This research was conducted under the sponsorship of the NASA Langley Research Center under Grant No. NSG 1248, the Army Research Office under Grant No. DAAG 29-77-G-0072, Project No. P14369-E and by the Office of Naval Research under Contract No. N00014-75-C-0511, Project No. NR 061-135.

** Professor, Dept. of Mechanical and Aerospace Engineering.

TABLE OF CONTENTS

1. Introduction and historicals

The object of the present paper is to introduce an explicit integration scheme for the Euler equations of gas dynamics which, after extensive tests, I consider the best among all schemes available so far.

According to P. Gordon, from whom I got the first suggestion of the scheme [1], its basic idea could be found in an early paper by Courant, Isaacson and Rees [2]. In 1967, after doing my homework on Gordon's scheme [3], I dropped it, giving my preference to MacCormack's scheme [4] which was also welcomed by a large number of numerical gas dynamicists.

Three reasons prompted me to adopt MacCormack's scheme instead of Gordon's:

1) The former has second order accuracy, the latter had only first order accuracy,

2) The former could be easily coded for any number of space-like variables, the latter was limited to one-dimensional problems, and, on a minor scale,

3) The former seemed to need simpler codes.

A couple of years ago, L. Zannetti rediscovered the basic idea of the integration scheme independently. He was, however, in a more advantageous position than Gordon because he had a good experience of two-level schemes and he knew how to maintain second order accuracy despite using one-sided approximations to space derivatives [5]. The first public appearance of Zannetti's scheme [6] showed that the first objection above had been removed; the scheme, however, was still essentially one-dimensional.

Since then, I have been working on the scheme, in order to test it in the widest possible range of flow parameters and

under the most exacting circumstances. I did also work out a multi-dimensional version of the scheme and I consider, thus, that the second objection above can also be removed. As far as the third objection is concerned, the code turned out to be not as complicated as I thought and it can be provided now in the form of a 'black box' which makes its application very simple.

Therefore, I believe that the scheme which I am going to describe deserves recognition. It is superior to any other from a physical standpoint and it provides results of great accuracy. The second statement is an obvious consequence of the first!

To identify the scheme, I decided to call it the λ-scheme, since I could not attribute to it a well-defined paternity. In fact, most of our recent progress in numerical analysis seems to be the product of a natural evolution, occurring in different places at almost the same pace. A paper by F. Walkden, P. Caine and G. T. Laws which just appeared in print [17], seems to overlap a good part of the present one although the Authors may have missed what I consider a very important improvement over the Gordon scheme. The scheme, as outlined by Walkden, has indeed only first order accuracy, and seems to make heavy use of averagings whose damaging influence cannot be evaluated a priori but which smell strongly of artificial viscosity.

2. Recasting of Euler's equations

In what follows, we will denote by T a time-like coordinate, and by X, Y two space-like coordinates. Such coordinates are in general not Cartesian, but obtained from Cartesian coordinates through a series of mappings and stretchings, as required by the problem.

As the main thermodynamical unknown we will assume the logarithm of pressure, P. In time-dependent problems, we will assume, as the main kinematic unknowns, the velocity components along the computational grid lines in the physical plane. In steady, supersonic flow problems, it is more convenient to assume

the slope of the velocity vector or two angles defining the velocity vector.

Beginning with one-dimensional problems, that is, problems which contain only one space-like variable, the typical unsteady flow is defined by the equations:

$$\begin{cases} P_T + a_{11}P_X + a_{12}u_X + c_1 = 0 \\ u_T + a_{21}P_X + a_{22}u_X + c_2 = 0 \end{cases} \qquad (1)$$

and the typical steady, supersonic flow is defined by similar equations, where u plays the role of the velocity slope. The coefficients, a_{ij} depend on the computational grid. The terms, c_i may also depend on other conditions or assumptions; for example, in unsteady flows c_1 is not zero if changes in a duct cross-sectional area are considered, c_2 is not zero if the frame of reference is accelerating.

The simplest possible case of unsteady flow is obtained if the frame of reference is fixed and Cartesian, if there are no area effects and no stretching of coordinates is used. In that case, for a perfect gas with a constant ratio of specific heats, γ, (1) become

$$\begin{cases} P_T + uP_X + \gamma u_X = 0 \\ u_T + \dfrac{a^2}{\gamma} P_X + uu_X = 0 \end{cases} \qquad (2)$$

Similarly, the simplest possible case of steady, supersonic flow is obtained if the frame of reference is fixed and Cartesian and no stretching of coordinates is used. In this case, if (for better clarity) we write σ instead of u for the slope of the velocity vector, and T and X are the horizontal and the vert-

ical Cartesian axes, respectively, (1) become

$$\begin{cases} P_T + (\sigma/\kappa)P_X + (\gamma/\kappa)\sigma_X = 0 \\ \sigma_T + (a^2/\gamma u^2)(1 + \sigma^2/\kappa)P_X + (\sigma/\kappa)\sigma_X = 0 \end{cases} \tag{3}$$

where u is the velocity component in the T-direction, and

$$\kappa = 1-a^2/u^2 \tag{4}$$

The slope of the characteristics of system (1) in the (X,Y) plane, $\lambda = dX/dT$, is obtained by solving the equation:

$$\begin{vmatrix} a_{11}-\lambda & a_{21} \\ a_{12} & a_{22}-\lambda \end{vmatrix} = 0 \tag{5}$$

There are, in general, two roots to this equation. We will denote by λ_1 and λ_2 the smaller and the larger root, respectively. It is well-known that the system (1) can be replaced by the equivalent system:

$$\begin{cases} (a_{22}-\lambda_1)(P_T+\lambda_1 P_X) - a_{12}(u_T+\lambda_1 u_X) + (a_{22}-\lambda_1)c_1 - a_{12}c_2 = 0 \\ (a_{22}-\lambda_2)(P_T+\lambda_2 P_X) - a_{12}(u_T+\lambda_2 u_X) + (a_{22}-\lambda_2)c_1 - a_{12}c_2 = 0 \end{cases} \tag{6}$$

Obviously, if the second equation (6) is subtracted from the first and the second equation, multiplied by $a_{22}-\lambda_1$, is subtracted from the first, multiplied by $a_{22}-\lambda_2$, we obtain (1) again. If, however, we write P_{X1} and u_{X1} for P_X and u_X in the first of (6) and, similarly, P_{X2} and u_{X2} in the second, we obtain

$$\begin{cases} P_T + A_1\lambda_1 P_{X1} - A_2\lambda_2 P_{X2} + D_{12}(\lambda_2 u_{X2} - \lambda_1 u_{X1}) + c_1 = 0 \\ u_T + D_{21}(\lambda_2 P_{X2} - \lambda_1 P_{X1}) + A_1\lambda_2 u_{X2} - A_2\lambda_1 u_{X1} + c_2 = 0 \end{cases} \tag{7}$$

where

$$A_i = \frac{a_{22}-\lambda_i}{\lambda_2-\lambda_1}, \qquad D_{ij} = \frac{a_{ij}}{\lambda_2-\lambda_1} \tag{8}$$

From the viewpoint of partial differential equations, $P_{X1} = P_{X2}$ and $u_{X1} = u_{X2}$; it is easy to verify that (7) are, once more, identical with (1). Not so from the viewpoint of finite difference equations, if we decide to approximate P_{X1} and P_{X2} in different ways, and similarly do with u_{X1} and u_{X2}.

Again, in the simple unsteady flow defined by (2),

$$a_{11} = u\ , \quad a_{12} = \gamma\ , \quad a_{21} = a^2/\gamma\ , \quad a_{22} = u$$
$$\lambda_1 = u-a\ , \qquad \lambda_2 = u+a \tag{9}$$

and (7) become

$$\begin{cases} P_T + \frac{1}{2}(\lambda_1 P_{X1} + \lambda_2 P_{X2}) + \frac{\gamma}{2a}(\lambda_2 u_{X2} - \lambda_1 u_{X1}) = 0 \\ u_T + \frac{a}{2\gamma}(\lambda_2 P_{X2} - \lambda_1 P_{X1}) + \frac{1}{2}(\lambda_2 u_{X2} + \lambda_1 u_{X1}) = 0 \end{cases} \tag{10}$$

whereas, in the simple supersonic flow defined by (3),

$$a_{11} = \sigma/\kappa\ , \ a_{12} = \gamma/\kappa\ , \ a_{21} = \frac{a^4\beta^2}{\gamma u^4\kappa}\ , \ a_{22} = \sigma/\kappa$$
$$\lambda_1 = \frac{1}{\kappa}(\sigma - \frac{a^2\beta}{u^2})\ , \ \lambda_2 = \frac{1}{\kappa}(\sigma + \frac{a^2\beta}{u^2})\ , \ \beta = \sqrt{M^2-1} \tag{11}$$

and (7) become

$$\begin{cases} P_T + \frac{1}{2}(\lambda_1 P_{X1} + \lambda_2 P_{X2}) - \frac{a^2\beta}{2\gamma u^2}(\lambda_2 \sigma_{X2} - \lambda_1 \sigma_{X1}) = 0 \\ \sigma_T + \frac{\gamma u^2}{2a^2\beta}(\lambda_2 P_{X2} - \lambda_1 P_{X1}) + \frac{1}{2}(\lambda_2 \sigma_{X2} + \lambda_1 \sigma_{X1}) = 0 \end{cases} \tag{12}$$

3. Discretization

From the two examples above, it is clear that λ_1 and λ_2 are the slopes of the two characteristics which carry the information necessary to define P and u (or P and σ) at every point. For such a point, A (Fig. 1) the domain of dependence is defined by point B and point C, the two characteristics being defined by AC and AB, respectively, to a first degree of accu-

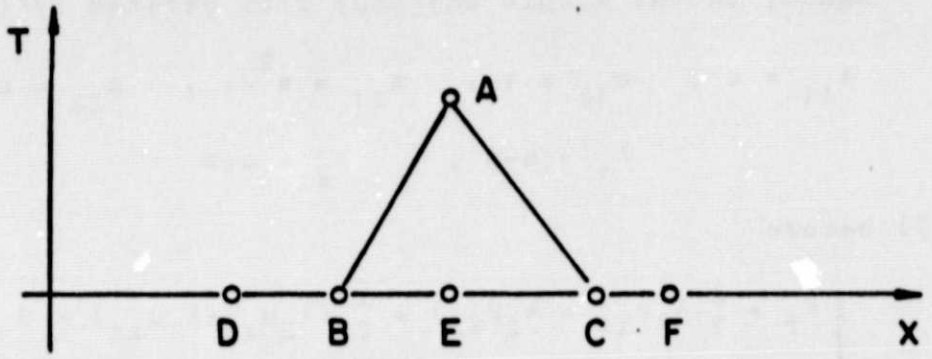

Fig. 1

racy. When discretizing the partial differential equations for computational purposes, point A must be made depend on points distributed on a segment which brackets BC [7], for example on points D,E and F of Fig. 1. Such a condition is necessary for stability but it must be interpreted with a grain of salt. Suppose, indeed, that one uses a scheme in which a point such as A is always made depend on D,E and F, indiscriminately (this is what happens in most of the schemes currently used, including the MacCormack scheme). Suppose, now, that the physical domain of dependence of A is the segment BC of Fig. 2. The information carried to A from F is not only unnecessary; it is undue and therefore the numerical scheme, whilst not violating the CFL rule, violates a law of physics, the law of forbidden signals. Physically, it would be much better to use only information from D and E to define A, even if this implied lowering the nominal degree of accuracy of the scheme. In other words, to say that a given scheme, using points D, E and F, has a second order accuracy is meaningless since a wrong scheme has no accura-

cy whatsoever.

In transonic problems treated by relaxation methods, the need for a switching in the discretization scheme in passing from subsonic to supersonic points was felt from the beginning [8], and it is evidently related to the law of forbidden signals, although we find it justified in the literature as a gimmick to avoid expansion shocks or to give the proper direction to the increase in entropy [9] (a curious statement, indeed, for a technique which is, by definition, isentropic!).

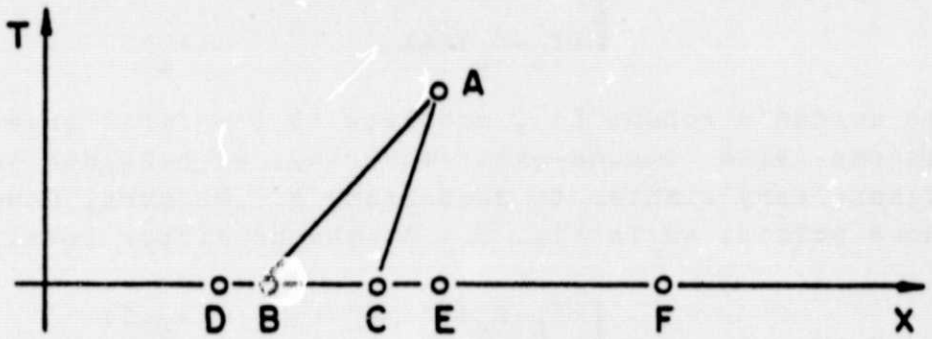

Fig. 2

The sensitivity of results to the numerical domain of dependence as related to the physical domain of dependence explains why computations which use integration schemes such as MacCormack's show a progressive deterioration as the AC line of Fig. 1 tends to become parallel to the T-axis ($\lambda_1 \to 0$), even if λ_1 is still negative [10]. The information from F actually does not reach A; in a coarse mesh, such information may be drastically different from the actual values (from C) which affect A. On the other hand, since the CFL rule must be satisfied and F is the nearest point to C on its right, the weight of such information should be minimized. The λ-scheme, relying on (7), provides us with such a possibility.

We stipulate that every derivative f_{x1} be approximated by using points which lie on the same side of E as C, and that every derivative f_{x2} be approximated by using points which lie on the same side of E as B. by so doing, not only we relate each characteristic with information which is found on

the same side of A from which the characteristic proceeds, but we weigh such information with factors which contain λ_1 and λ_2 so that the contribution of points located too far outside the physical domain of dependence is minimized.

A one-level scheme which defines

$$f_{Xi} = \begin{cases} (f_F - f_E)/\Delta X & (\lambda_i < 0) \\ \\ (f_E - f_D)/\Delta X & (\lambda_i > 0) \end{cases} \tag{13}$$

is Gordon's scheme [1], accurate to the first order. To obtain a scheme with second-order accuracy, we consider two levels, in a manner very similar to MacCormack's. We must, however, introduce more points, as in Fig. 3. At the predictor level, we define

$$f_{Xi} = \begin{cases} (f_F - f_E)/\Delta X & (\lambda_i < 0) \\ \\ (2f_E - 3f_D + f_G)/\Delta X & (\lambda_i > 0) \end{cases} \tag{14}$$

At the corrector level, we define

$$f_{Xi} = \begin{cases} (-2f_A + 3f_N - f_P)/\Delta X & (\lambda_i < 0) \\ \\ (f_A - f_M)/\Delta X & (\lambda_i > 0) \end{cases} \tag{15}$$

It is easy to see that, if any function f is updated as

$$\bar{f} = f + f_T \Delta T \tag{16}$$

at the predictor level, with the T-derivatives defined as in (7) and the X-derivatives defined as in (14), and as

$$f(T + \Delta T) = \frac{1}{2}(f + \bar{f} + \bar{f}_T \Delta T) \tag{17}$$

at the corrector level, with the T-derivatives defined again as in (7) and the X-derivatives defined as in (15), the value of f at T + ΔT is obtained with second order accuracy. The updating

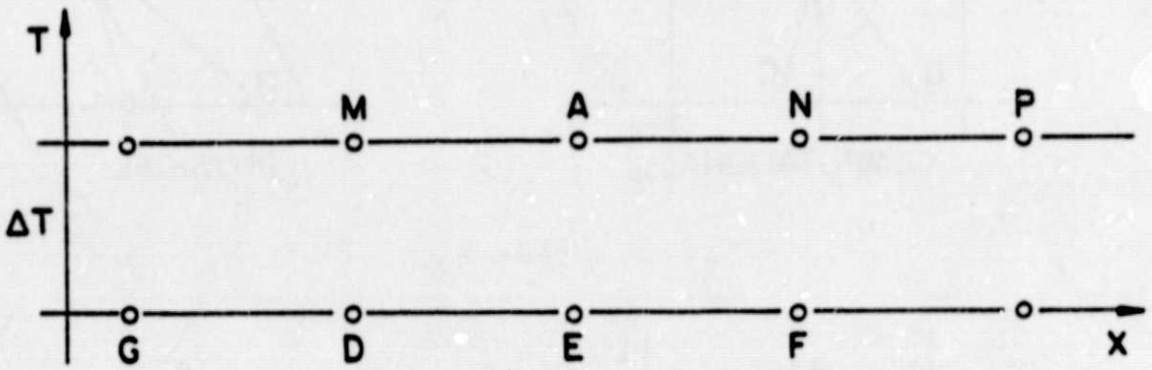

Fig. 3

rules (16) and (17) are the same as in the MacCormack scheme.

4. Additional remarks and a 'black box' sample

In the simple examples above, the computational grid coincides with the physical grid, which is fixed. The characteristics are the physical characteristics of the flow. For example, in the unsteady case, the domains of dependence are related to the simple concept of subsonic flow (for $u>0$, $u<a$, $\lambda_1<0, \lambda_2>0$) and supersonic flow ($u>a$, $\lambda_1>0, \lambda_2>0$); similarly, in the case $u<0$. The system (1), however, as well as (7), is much more general. The computational grid, in the (X, T) plane, is fixed but its counterpart in the physical plane generally varies with T. The discussion of the domain of dependence is carried on and the slope of the characteristics is determined in the (X,T) plane, with reference to the fixed grid. Therefore, it may happen that a flow which is physically supersonic has to be considered as 'subsonic' in the computation (Fig. 4); conversely, a physically subsonic flow may have to be considered as 'supersonic' in the computation (Fig. 5).

We conclude our analysis of the λ-scheme by showing (in Fig. 6) an example of a FORTRAN subroutine to compute the X-

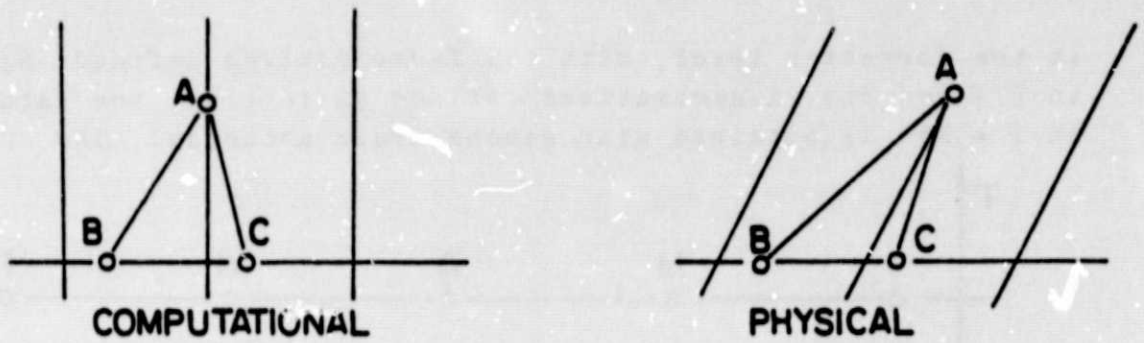

Fig. 4

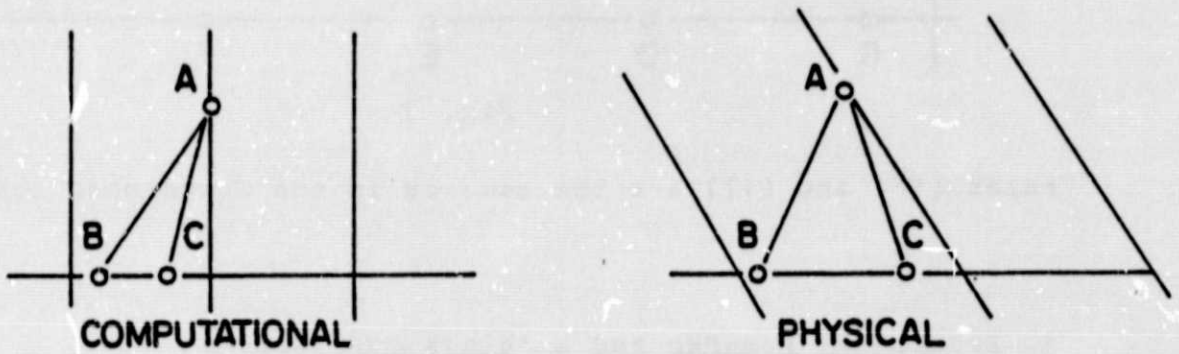

Fig. 5

derivatives according to the conventions outlined above. There, LOOP=-1, + 1 in the predictor and corrector stage, respectively, N denotes the grid point location, LAP=(LOOP + 1)/2, and ALAM(1), ALAM(2) are $-\lambda_1$ and λ_2, respectively. Special provisions are made at N=1,2 and at N=NA, NC where NC is the last grid point and NA=NC-1 to account, in this case, for the presence of two rigid walls.

5. The equation of energy

The equation of energy is conspicuously absent from our analysis, so far. Indeed, written in terms of entropy, it simply states the invariance of S on a particle path:

```
      I=1
      NTL=N-LOOP
      LX=LAP+1
      LX1=3-LX
      N0=N-LOOP
      N1=N+LOOP
      N2=N1+LOOP
      PN=P(N)
      UN=U(N)
      PN0=P(N0)
      UN0=U(N0)
      PN1=P(N1)
      UN1=U(N1)
      PN2=P(N2)
      UN2=U(N2)
      IF(NTL.NE.-2.AND.NTL.NE.NA)GO TO 9
      PN2=3.*(PN1-PN)+PN0
      UN2=3.*(UN1-UN)+UN0
    9 IF(ALAM(LX).LT.0)GO TO 1
      IF(NTL.EQ.1.OR.NTL.EQ.-NC)GO TO 3
      PX(LX)=(PN-PN0)*DDXD
      UX(LX)=(UN-UN0)*DDXD
      IF(NTL.EQ.-1.OR.NTL.EQ.NC)GO TO 7
      IF(ALAM(LX1).LT.0.)GO TO 7
      LSAV=LX
      LX=LX1
      LX1=LSAV
    1 I=LX+LAP
    3 PX(LX)=(-2.*PN+3.*PN1-PN2)*DDXD
      UX(LX)=(-2.*UN+3.*UN1-UN2)*DDXD
      IF(I.EQ.2)RETURN
    7 PX(LX1)=PX(LX)
      UX(LX1)=UX(LX)
      RETURN
```

Fig. 6

$$DS/Dt=0 \tag{18}$$

where t is real time (In the two simple examples above, (18) becomes

$$S_T + uS_X=0 \tag{19}$$

and

$$S_T + \sigma S_X=0 \tag{20}$$

respectively).

At each integration step, the other equations of motion can and should be integrated independently of (18); the latter, in turn, should be integrated by approximating the X-derivative of S in such a way that information is never carried backwards on a particle path [11]. Obviously, the rules for the approximation of S_X are different from the rules for the approximation

of P_X, u_X, σ_X, and any conceptual or coding mixup should be carefully avoided. The only interaction between entropy and the other dependent variables of a flow problem occurs via the value of a^2 in unsteady flows (see(2)) or a^2, u^2, κ in steady flows (see (3)) since, in general,

$$a^2 = \gamma \exp[(\gamma-1)P/\gamma + S/\gamma] \tag{21}$$

and, for steady flows,

$$q^2 = \frac{2}{\gamma-1}(a_o^2 - a^2) \tag{22}$$

where a_o is the stagnation speed of sound, and q is the modulus of the velocity.

6. Extension to multidimensional problems. Unsteady flows

Let us consider now a problem with two space-like variables, X and Y. The typical unsteady flow is described by the equations:

$$\begin{cases} P_T + a_{11}P_X + a_{12}u_X + b_{11}P_Y + b_{12}v_Y + g_{11}u_Y + g_{12}v_X + c_1 = 0 \\ u_T + a_{21}P_X + a_{22}u_X + h_{21}P_Y + h_{22}v_Y + d_2u_Y + g_{22}v_X + c_2 = 0 \\ v_T + h_{31}P_X + h_{32}u_X + b_{21}P_Y + b_{22}v_Y + g_{31}u_Y + d_3v_X + c_3 = 0 \end{cases} \tag{23}$$

The simplest possible case of unsteady flow is obtained if the gas is perfect, the frame of reference is fixed and Cartesian, and no stretching of coordinates is used. In that case, (23) become

$$\begin{cases} P_T + uP_X + vP_Y + \gamma u_X + \gamma v_Y = 0 \\ u_T + uu_X + vu_Y + (a^2/\gamma)P_X = 0 \\ v_T + uv_X + vv_Y + (a^2/\gamma)P_Y = 0 \end{cases} \tag{24}$$

We see that not only the c_i terms but also the terms affected by the coefficients g_{ij} and h_{ij} depend on the choice of the computational grid. For a well-chosen grid, we expect such terms to play a minor role in the computation. Most of the remaining terms can be arranged in two matrices, one formed with X-derivatives of P and u, the other with Y-derivatives of P and v. Two terms are left out, $d_2 u_Y$ and $d_3 v_X$, which, as seen from (24), are physically relevant.

We will now rearrange the equations (23) in two sets, one essentially related to X and the other essentially related to Y:

$$\begin{cases} P_T^X + a_{11}P_X + a_{12}u_X + g_{11}u_Y + c_1 = 0 \\ u_T + a_{21}P_X + a_{22}u_X + d_2 u_Y + h_2 P_Y + c_2 = 0 \end{cases} \tag{25}$$

and

$$\begin{cases} P_T^Y + b_{11}P_Y + b_{12}v_Y + g_{12}v_X = 0 \\ v_T + b_{21}P_Y + b_{22}v_Y + d_3 v_X + h_3 P_X + c_3 = 0 \end{cases} \tag{26}$$

The meaning of P_T^X and P_T^Y is simply that P_T, in (23), is intended to be obtained as the sum of two separate contributions, P_T^X and P_T^Y; therefore, if the first of (25) and the first of (26) are added together, one obtains the first of (23) again. The distribution of the terms, $g_{11}u_Y$, $g_{22}v_X$ and c_i, between the first of (25) and the first of (26) is arbitrary, but the arbitrariness is irrelevant, as we will see soon.

Both (25) and (26) show a strong resemblance to (1), particularly if we rewrite them in the form

$$\begin{cases} P_T^X + a_{11}P_X + a_{12}u_X + C_1^X = 0 \\ u_T + a_{21}P_X + a_{22}u_X + C_2^X = 0 \end{cases} \tag{27}$$

and

$$\begin{cases} P_T^Y + b_{11}P_Y + b_{12}v_Y + C_1^Y = 0 \\ v_T + b_{21}P_Y + b_{22}v_Y + C_2^Y = 0 \end{cases} \tag{28}$$

with

$$\begin{aligned} C_1^X &= g_{11}u_Y + c_1 \ , \quad C_2^X = d_2 u_Y + h_2 P_Y + c_2 \\ C_1^Y &= g_{12}v_X \ , \quad C_2^Y = d_3 v_X + h_3 P_X + c_3 \end{aligned} \tag{29}$$

Therefore, we can proceed as in Section 2 for (27) and (28), separately, to obtain two sets of equations similar to (7):

$$\begin{cases} P_T^X + A_1\lambda_1^X P_{X1} - A_2\lambda_2^X P_{X2} + D_{12}^X(\lambda_2^X u_{X2} - \lambda_1^X u_{X1}) + C_1^X = 0 \\ u_T + D_{21}^X(\lambda_2^X P_{X2} - \lambda_1^X P_{X1}) + A_1\lambda_2^X u_{X2} - A_2\lambda_1^X u_{X1} + C_2^X = 0 \end{cases} \tag{30}$$

and

$$\begin{cases} P_T^Y + B_1\lambda_1^Y P_{Y1} - B_2\lambda_2^Y P_{Y2} + D_{12}^Y(\lambda_2^Y v_Y 2 - \lambda_1^Y v_Y 1) + C_1^Y = 0 \\ v_T + D_{21}^Y(\lambda_2^Y P_{Y2} - \lambda_1^Y P_{Y1}) + B_1\lambda_2^Y v_Y 2 - B_2\lambda_1^Y v_Y 1 + C_2^Y = 0 \end{cases} \tag{31}$$

where

$$\begin{aligned} A_i &= \frac{a_{22} - \lambda_i^X}{\lambda_2^X - \lambda_1^X} \ , \quad B_i = \frac{b_{22} - \lambda_i^Y}{\lambda_2^Y - \lambda_1^Y} \\ D_{ij}^X &= \frac{a_{ij}}{\lambda_2^X - \lambda_1^X} \ , \quad D_{ij}^Y = \frac{b_{ij}}{\lambda_2^Y - \lambda_1^Y} \end{aligned} \tag{32}$$

and λ_i^X, λ_i^Y are solutions of equations similar to (5):

$$\begin{vmatrix} a_{11}-\lambda_i^X & a_{21} \\ a_{12} & a_{22}-\lambda_i^X \end{vmatrix} = 0 \ , \quad \begin{vmatrix} b_{11}-\lambda_i^Y & b_{21} \\ b_{12} & b_{22}-\lambda_i^Y \end{vmatrix} = 0 \qquad (33)$$

In discretizing (30) and (31), we will use the same rules as stated in Section 4.

We turn our attention now to the discretization of the X- and Y-derivatives in (29). The most important terms, u_Y in C_2^X and v_X in C_2^Y, should be discretized recalling that they come from Lagrangian derivatives in momentum equations. Therefore, it seems proper to discretize them the same way the entropy derivatives are approximated in the energy equation. Specifically, the sign of d_3 must be tested; then, at the predictor level,

$$v_X = \begin{cases} (v_F - v_E)/\Delta X & (d_3 < 0) \\ \\ (2v_E - 3v_D - v_G)/\Delta X & (d_3 > 0) \end{cases} \qquad (34)$$

and, at the corrector level,

$$v_X = \begin{cases} (-2v_A + 3v_N - v_P)/\Delta X & (d_3 < 0) \\ \\ (v_A - v_M)/\Delta X & (d_3 > 0) \end{cases} \qquad (35)$$

Similar formulas are used for u_Y, with reference to the sign of d_2. The same approximations can be used for the derivatives appearing in C_1^X and C_1^Y. We recall that they are affected by coefficients which should be small; therefore, any approximation should serve the purpose. For the same reason, any approximation to P_X and P_Y appearing in the grid corrective terms in C_2^X and C_2^Y should work. One can choose to use centered differences or a

MacCormack-type of alternating backward and forward differences.

Once P_T^X and P_T^Y have been evaluated, P_T may be obtained as

$$P_T = P_T^X + P_T^Y \tag{36}$$

Obviously, the same result is obtained by coding P_T in one single equation:

$$\begin{aligned} &P_T + A_1\lambda_1^X P_{X1} - A_2\lambda_2^X P_{X2} + B_1\lambda_1^Y P_{Y1} - B_2\lambda_2^Y P_{Y2} + \\ &+ D_{12}^X(\lambda_2^X u_{X2} - \lambda_1^X u_{X1}) + D_{12}^Y(\lambda_2^Y v_{Y2} - \lambda_1^Y v_{Y1}) + C_1 = 0 \end{aligned} \tag{37}$$

This shows that the scheme does not belong to the class of fractional step schemes [12,13]. The initial separation of the equations was introduced to allow two independent sets of characteristics to be defined, one in the (X, T) plane and the other in the (Y, T) plane. Attempts of the late fifties and early sixties to define and use an optimal set of three-dimensional characteristics proved to be cumbersome, difficult to apply and, at times, unstable or inaccurate. The present approach may not be appealing from a formal viewpoint but it fulfills the purpose of defining the domain of dependence of the point to be evaluated as far as pressure and any other variable having the same domain of dependence as the pressure are concerned.

7. Three-dimensional, steady, supersonic flows

Three-dimensional, steady, supersonic flows must be treated in a different way, although the basic concepts remain unaltered. This is because the physical nature of the three independent variables is the same, despite one playing a time-like role. We begin by observing that, after introducing two angular variables, σ and η, defining the direction of the velocity vector, the Euler equations can be written in the matrix form:

$$f_T + Af_X + Bf_Y + c - kP_T = 0 \tag{38}$$

where

$$f=\begin{bmatrix}P\\ \sigma\\ \eta\end{bmatrix},\quad A=\begin{bmatrix}a_{11} & a_{12} & a_{13}\\ a_{21} & a_{22} & 0\\ a_{31} & 0 & a_{22}\end{bmatrix},\quad B=\begin{bmatrix}b_{11} & b_{12} & b_{13}\\ b_{21} & b_{22} & 0\\ b_{31} & 0 & b_{22}\end{bmatrix},\quad c=\begin{bmatrix}c_1\\ c_2\\ c_3\end{bmatrix},\quad k=\begin{bmatrix}0\\ k_2\\ k_3\end{bmatrix} \tag{39}$$

We can split the system (38) into two systems:

$$\begin{cases} P_T^X + a_{11}P_X + a_{12}\sigma_X + a_{13}\eta_X + c_1 = 0\\ \sigma_T^X + a_{21}P_X + a_{22}\sigma_X + c_2 - k_2P_T^X = 0\\ \eta_T^X + a_{31}P_X + a_{22}\eta_X + c_3 - k_3P_T^X = 0 \end{cases} \tag{40}$$

and

$$\begin{cases} P_T^Y + b_{11}P_Y + b_{12}\sigma_Y + b_{13}\eta_Y = 0\\ \sigma_T^Y + b_{21}P_Y + b_{22}\sigma_Y - k_2P_T^Y = 0\\ \eta_Y + b_{31}P_Y + b_{22}\eta_Y - k_3P_T^Y = 0 \end{cases} \tag{41}$$

so that, if each equation (40) is added to its counterpart in (41), (38) is obtained again, provided that

$$P_T = P_T^X + P_T^Y,\quad \sigma_T = \sigma_T^X + \sigma_T^Y,\quad \eta_T = \eta_T^X + \eta_T^Y \tag{42}$$

For each new system two values of λ can be found, defined by

$$(\lambda_i^X)^2-(a_{11}+a_{22}+a_{13}k_3+a_{12}k_2)\lambda_i^X+(a_{11}a_{22}-a_{13}a_{31}-a_{12}a_{21})=0 \tag{43}$$

and

$$(\lambda_i^Y)^2-(b_{11}+b_{22}+b_{13}k_3+b_{12}k_2)\lambda_i^Y+(b_{11}b_{22}-b_{13}b_{31}-b_{12}b_{21})=0 \tag{44}$$

respectively, and a third value, defined by

$$\lambda_3^X=a_{22} \tag{45}$$

and

$$\lambda_3^Y = b_{22} \tag{46}$$

respectively. The direction defined by λ_3 plays the role of a streamline in (X,T) plane or the (Y,T) plane. Non-trivial sets of multipliers can be found in connection with each of the λ_i to build two sets of compatibility equations. Specifically,

$$\begin{cases} \mu_{i1}^X = a_{22} - \lambda_i^X \\ \mu_{i2}^X = -a_{12} \\ \mu_{i3}^X = -a_{13} \end{cases} \qquad \begin{cases} \mu_{i1} = b_{22} - \lambda_i^Y \\ \mu_{i2}^Y = -b_{12} \\ \mu_{i3}^Y = -b_{13} \end{cases} \tag{47}$$

for i=1,2, and

$$\begin{cases} \mu_{31}^X = 0 \\ \mu_{32}^X = -(a_{31} + k_3 a_{22}) \\ \mu_{33}^X = a_{21} + k_2 a_{22} \end{cases} \qquad \begin{cases} \mu_{31}^Y = 0 \\ \mu_{32}^Y = -(b_{31} + k_3 b_{22}) \\ \mu_{33}^Y = b_{21} + k_2 b_{22} \end{cases} \tag{48}$$

The compatibility equations, in which we write f_{Xi} and f_{Yi} instead of f_X and f_Y (see Section 2), are

$$\begin{cases} \alpha^X (P_T^X + \lambda_1^X P_{X1}) - a_{12}(\sigma_T^X + \lambda_1^X \sigma_{X1}) - a_{13}(\eta_T^X + \lambda_1^X \eta_{X1}) + \Sigma \mu_{1j}^X c_j = 0 \\ -\alpha^X (P_T^X + \lambda_2^X P_{X2}) - a_{12}(\sigma_T^X + \lambda_2^X \sigma_{X2}) - a_{13}(\eta_T^X + \lambda_2^X \eta_{X2}) + \Sigma \mu_{2j}^X c_j = 0 \\ -\delta^X (P_T^X + a_{22} P_{X3}) + \mu_{32}^X (\sigma_T^X + a_{22} \sigma_{X3}) + \mu_{33}^X (\eta_T^X + a_{22} \eta_{X3}) + \Sigma \mu_{3j}^X c_j = 0 \end{cases} \tag{49}$$

where

$$\alpha^X = \mu_{11} - \mu_{12} k_2 - \mu_{13} k_3 \quad , \quad \delta^X = a_{21} k_3 - a_{31} k_2 \tag{50}$$

Similar equations can be written with respect to Y. From the

first two equations (49) we get one equation for P_T^X:

$$2a^X P_T^X + a^X(\lambda_1^X P_{X1} + \lambda_2^X P_{X2}) - a_{12}(\lambda_1^X \sigma_{X1} - \lambda_2^X \sigma_{X2}) - \tag{51}$$
$$-a_{13}(\lambda_1^X \eta_{X1} - \lambda_2^X \eta_{X2}) + (\lambda_2^X - \lambda_1^X)c_1 = 0$$

and another equation for the unknown ϕ^X :

$$-2\phi^X + a^X(\lambda_1^X P_{X1} - \lambda_2^X P_{X2}) - a_{12}(\lambda_1^X \sigma_{X1} + \lambda_2^X \sigma_{X2}) - \tag{52}$$
$$-a_{13}(\lambda_1^X \eta_{X1} + \lambda_2^X \eta_{X2}) + \Sigma(\mu_{1j}^X + \mu_{2j}^X)c_j = 0$$

where

$$\phi^X = a_{12}\sigma_T^X + a_{13}\eta_T^X \tag{53}$$

Finally, considering P_T^X as defined by (51), the third of (49) yields

$$\psi^X - \delta^X(P_T^X + a_{22}P_{X3}) + \mu_{32}^X a_{22}\sigma_{X3} + \mu_{33}^X a_{22}\eta_{X3} + \Sigma\mu_{3j}^X c_j = 0 \tag{54}$$

where

$$\psi^X = \mu_{32}^X \sigma_T^X + \mu_{33}^X \eta_T^X \tag{55}$$

and σ_T^X, η_T^X can be obtained by solving the system (53),(55). One should proceed in a similar way for the second set (41) and then apply (42) to get P_T, σ_T and η_T.

The rules for discretization are the same as outlined in Section 3. The f_{X3} and f_{Y3} approximations coincide with f_{X1} and f_{Y1} if the signs of $^X\lambda_3$ and $^Y\lambda_3$ coincide; otherwise, they will coincide with f_{X2} and f_{Y2}.

In the simple case of Cartesian coordinates with no

stretching,

$$\begin{cases} a_{11}=\sigma/\kappa, & a_{12}=\gamma/\kappa, & a_{13}=0 \\ a_{21}=a^2/\gamma w^2, & a_{22}=\sigma, & a_{23}=0, \quad k_2=a_{21}\sigma \\ a_{31}=0, & a_{32}=0, & a_{33}=\sigma, \quad k_3=a_{21}\eta \end{cases} \tag{56}$$

$$\begin{cases} b_{11}=\eta/\kappa, & b_{12}=0, & b_{13}=\gamma/\kappa \\ b_{21}=0, & b_{22}=\eta, & b_{23}=0, \quad k_2=a_{21}\sigma \\ b_{31}=a_{21}, & b_{32}=0, & b_{33}=\eta, \quad k_3=a_{21}\eta \end{cases} \tag{57}$$

and all $c_i=0$. Then,

$$\begin{cases} \lambda_i^X=(\sigma\pm\beta^X)/\kappa, \quad \beta^X=\dfrac{a^2}{w^2}\left[w^2(1+\sigma^2)/a^2-1\right]^{1/2} \\ \\ \lambda_i^Y=(\eta\pm\beta^Y)/\kappa, \quad \beta^Y=\dfrac{a^2}{w^2}\left[w^2(1+\eta^2)/a^2-1\right]^{1/2} \end{cases} \tag{58}$$

$$\begin{cases} \mu_{i1}^X=\sigma-\lambda_i^X & \mu_{i1}^Y=\eta-\lambda_i^Y \\ \mu_{i2}^X=-\gamma/\kappa & \mu_{i2}^Y=0 \\ \mu_{i3}^X=0 & \mu_{i3}^Y=-\gamma/\kappa \end{cases} \tag{59}$$

for i=1,2, and

$$\begin{cases} \mu_{31}^X=0 & \mu_{31}^Y=0 \\ \mu_{32}^X=-a_{21}\eta\sigma & \mu_{32}^Y=-a_{21}(\eta^2+1) \\ \mu_{33}^X=a_{21}(\sigma^2+1) & \mu_{33}^Y=a_{21}\eta\sigma \end{cases} \tag{60}$$

so that

$$\alpha^X = \beta^X/\kappa \quad , \quad \alpha^Y = \beta^Y/\kappa \tag{61}$$

$$\phi^X = \gamma\sigma\sigma_T^X/\kappa \quad , \quad \phi^Y = \gamma n\sigma_T^Y/\kappa \tag{62}$$

$$\psi^X = \frac{a^2}{\gamma w^2}[(\sigma^2 + 1)n_T^X - \sigma n\sigma_T^X], \quad \psi^Y = \frac{a^2}{\gamma w^2}[\sigma n n_T^Y - (n^2 + 1)\sigma_T^Y] \tag{63}$$

All complications appearing in the general formulation above depend on the geometry of the computational grid and should not be relevant from a physical viewpoint.

8. Tests and results

Some examples should make clear the ability of the scheme to represent difficult transonic flows. We will begin with two one-dimensional cases, one of which is unsteady and the other steady and supersonic.

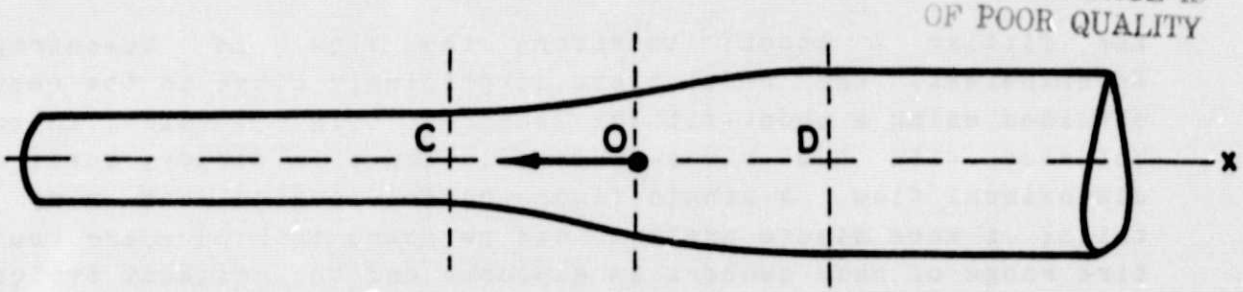

Fig. 7

The first example is illustrated in Fig. 8, which shows the Mach number distribution over a stretch of an infinite duct having a variable cross-section (Fig. 7). In the portion of the pipe considered in the figure the flow, which started from rest and passed through an unsteady evolution, has already reached a steady state. A shock was originated and moved to a final steady position. The calculation used to get Fig. 8 has no provision

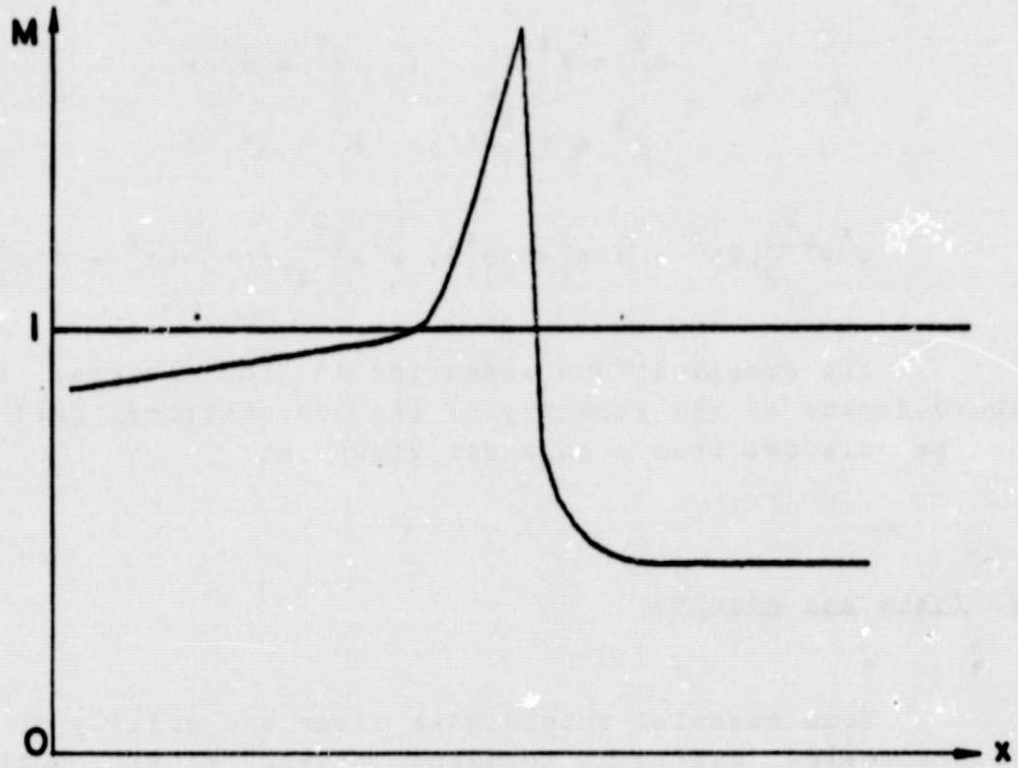

Fig. 8

for fitting a shock; therefore the flow is homentropic. Nevertheless, the results are surprisingly close to the results obtained using a shock-fitting technique (Fig. 9) which, in turn, coincide with the close-form solution of a steady, quasi-one-dimensional flow. A single figure cannot provide too many details; a more minute analysis can be found in [10] where the entire range of Mach numbers is explored and the unsteady evolution leading to the asymptotic steady state is analyzed. I would like to warn the reader against concluding, from a glance to Fig. 8, that the λ-scheme has shock-capturing virtues; such a feat is made impossible by the inability of the scheme to provide entropy jumps. It is undoubtedly true, however, that the scheme remains stable and accurate under very exacting transonic circumstances, even when the computational mesh is very coarse; in Fig. 10 asymptotic results obtained with the mesh of Fig. 8 and a much coarser mesh are shown, and no deterioration can be observed.

The second example is illustrated in Fig. 11, which shows the Mach number distribution in a channel opening into vacuum.

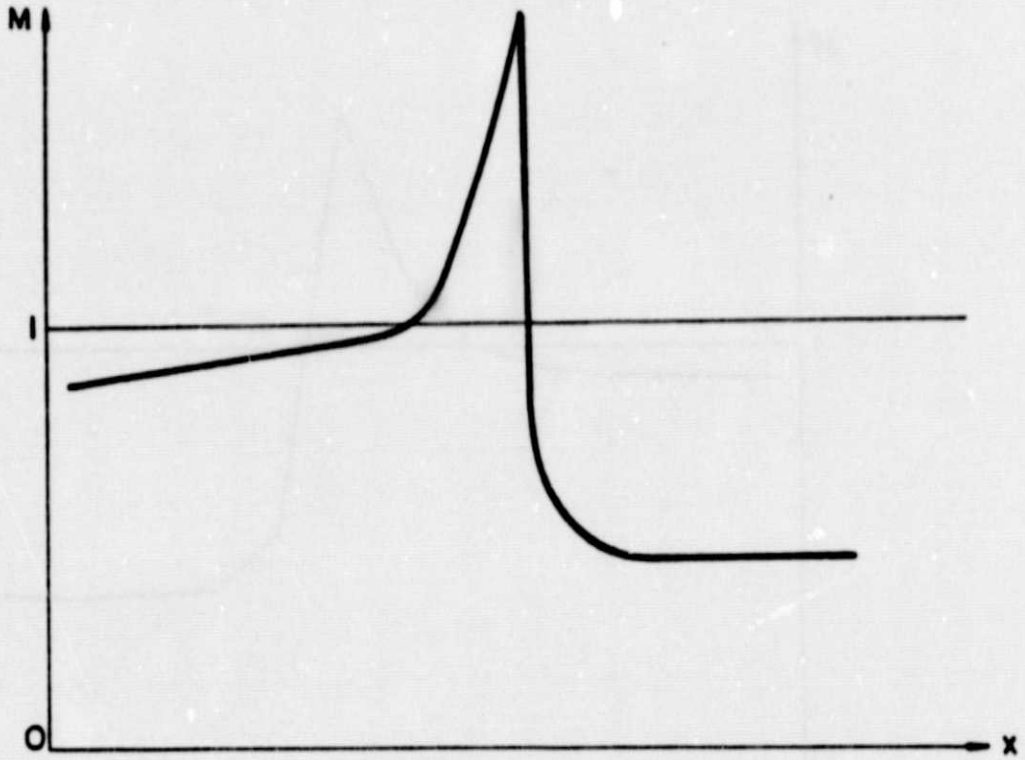

Fig. 9

The flow at the channel inlet is uniform; its Mach number equals 1.04. The calculation [14] is performed advancing on a grid of which Fig. 12 shows typical lines. On each grid line crossing the channel, 21 points are considered. In this case, the accuracy of the scheme and its ability to handle difficult situations is demonstrated by the perfect splitting of the computed flow into two regions, a simple wave adjacent to the lower wall and a source-like pattern in the rest of the channel. Such a splitting is due to the fact that no down-running characteristic can reach the lower wall. In Fig. 11, line AB is the first significant down-running characteristic.

An impressive example of the ability of the scheme to handle two-dimensional, unsteady flows is shown in Fig. 13. In it, we see the steady shock-and-isobars pattern reached asymptotically about an ablated blunt body via an unsteady calculation. The free stream Mach number is 12. The computational grid (wrapped around the body by conformal mapping [15]) has 30 intervals along the body and 15 intervals between body and shock. In

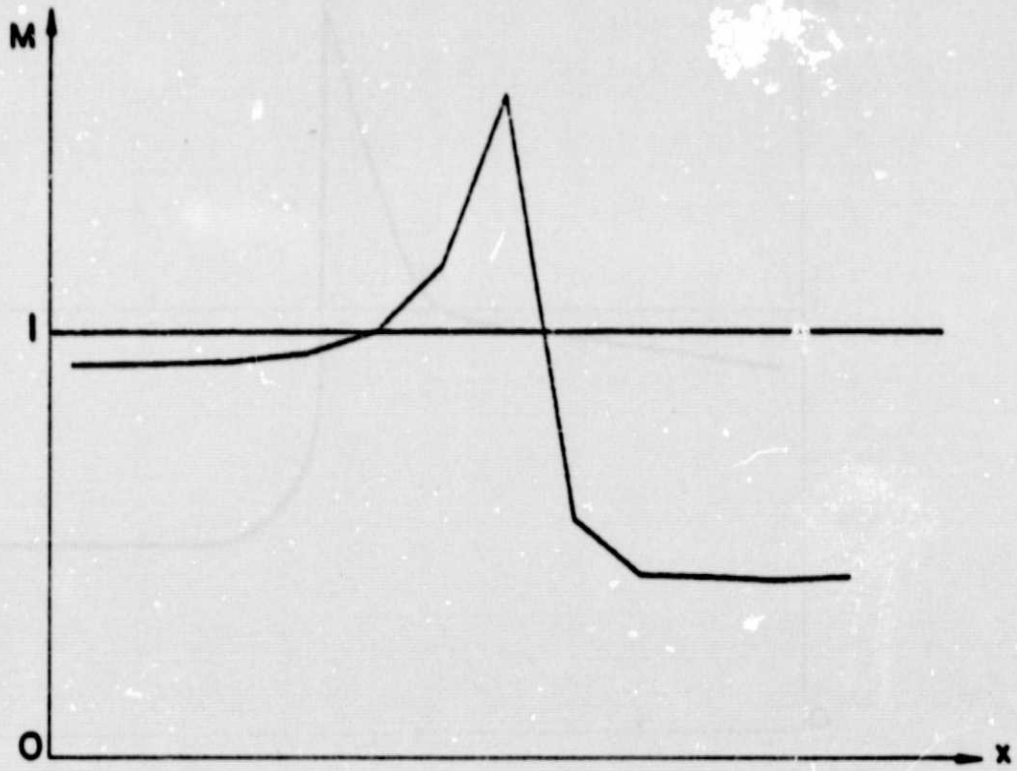

Fig. 10

the figure, in addition to isobars, two sonic lines are shown. A thin subsonic layer appears in the concavity of the body. The bow shock shape matches the one obtained experimentally [16].

Finally, an example is given of the application of the technique to three-dimensional, steady, supersonic flows. In Fig. 14 the bow shock and the isobar pattern about an elliptic cone, with a 14:1 axis ratio and a leading edge angle of 20° are shown. The free stream Mach number is 2 and the angle of attack is equal to 5°. Despite the coarseness of the computational mesh (24 intervals around the body and 12 between body and bow shock) the pressure distribution on the body is remarkably accurate, as shown in Fig. 15. The results are part of an extensive series of tests involving vehicle shapes of increasing complexity, to be published in the near future.

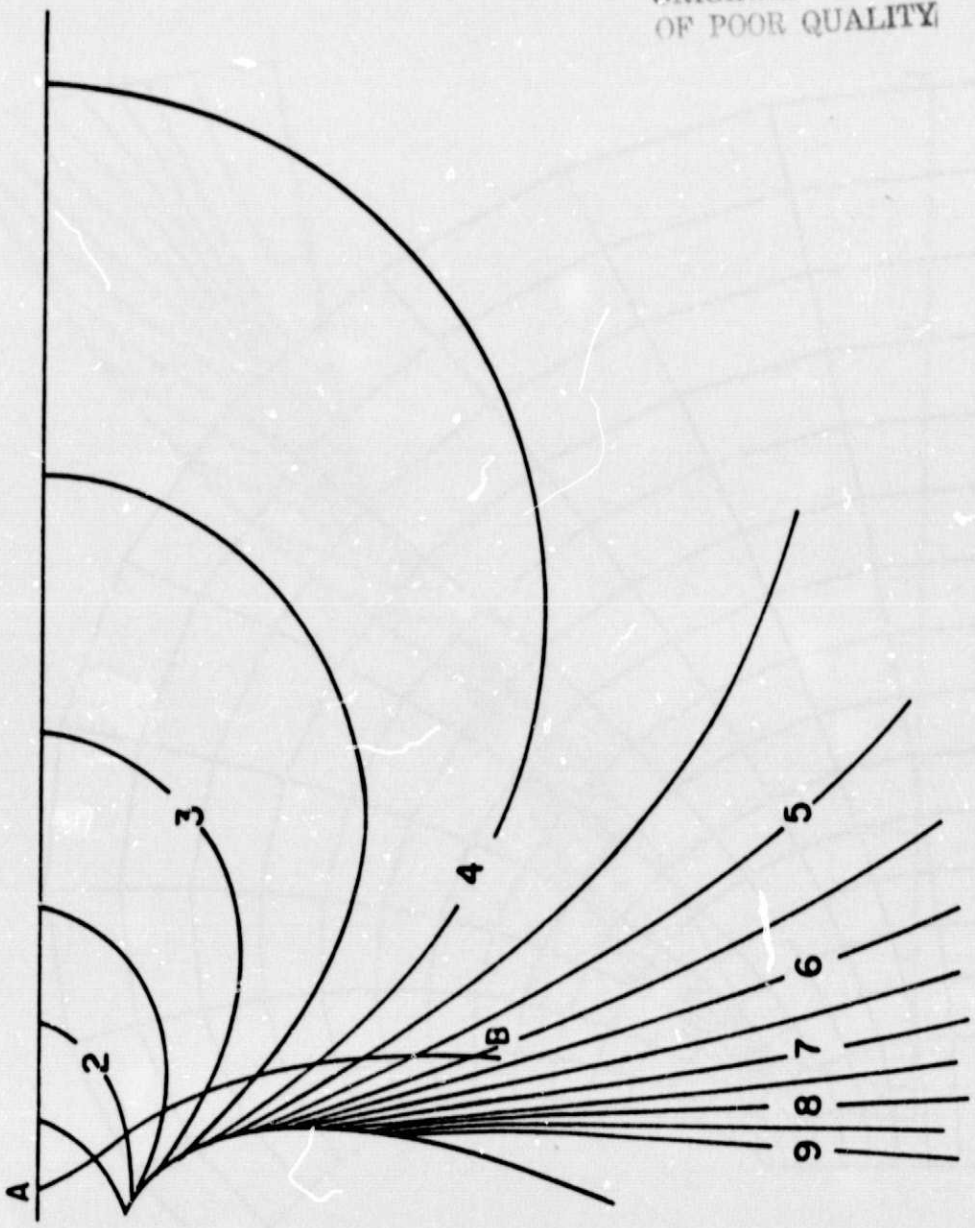

Fig. 11

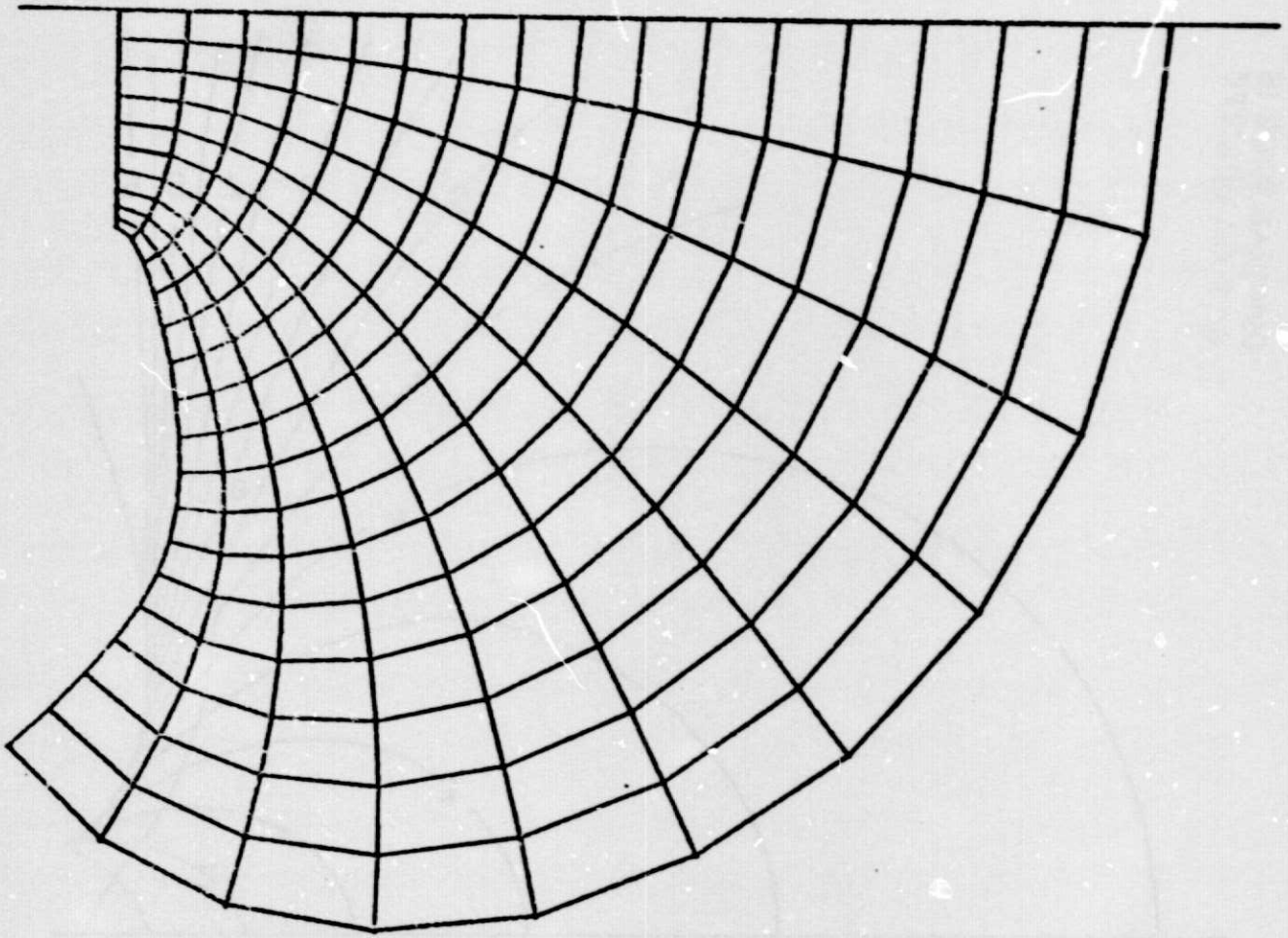

Fig. 12

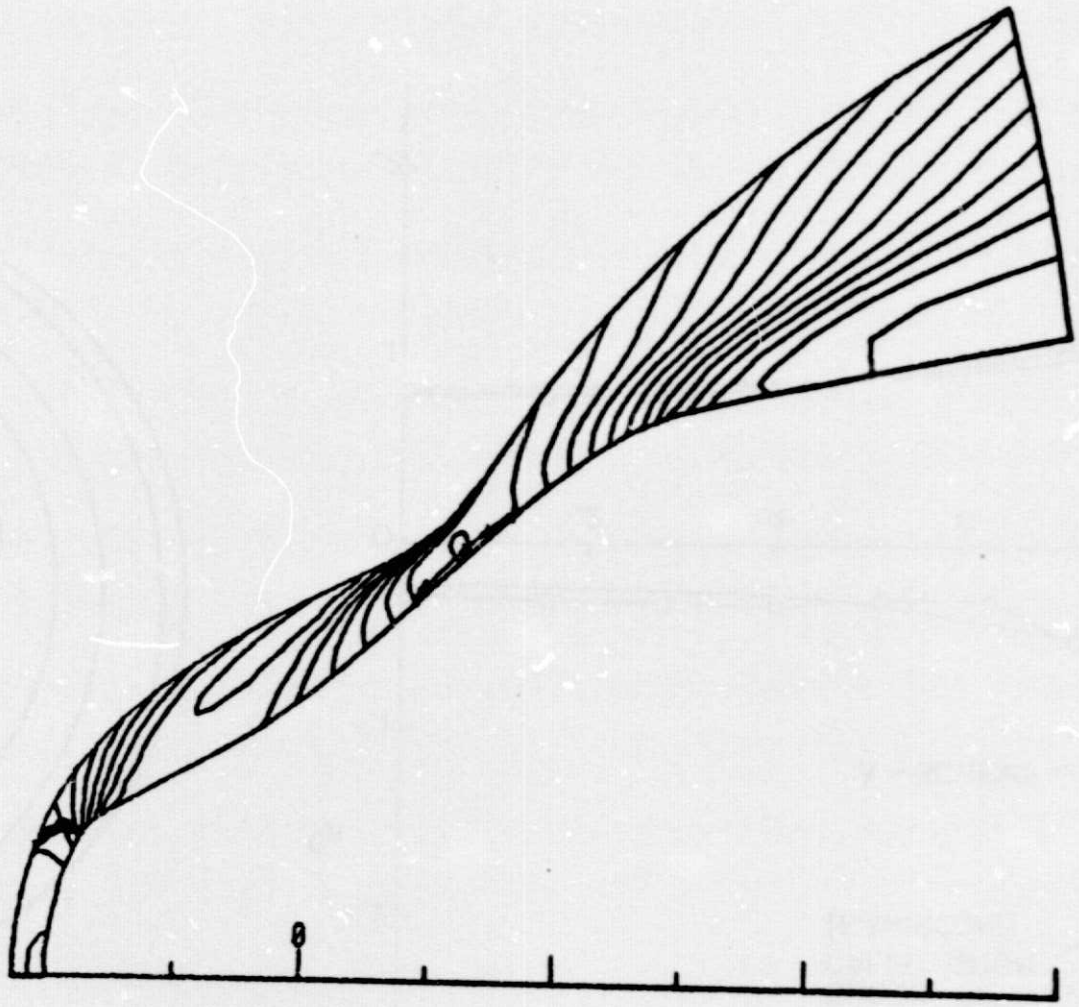

Fig. 13

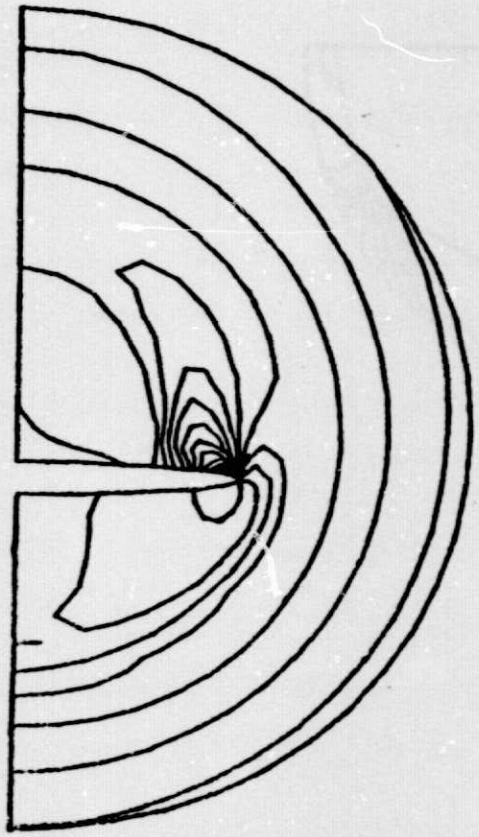

Fig. 14

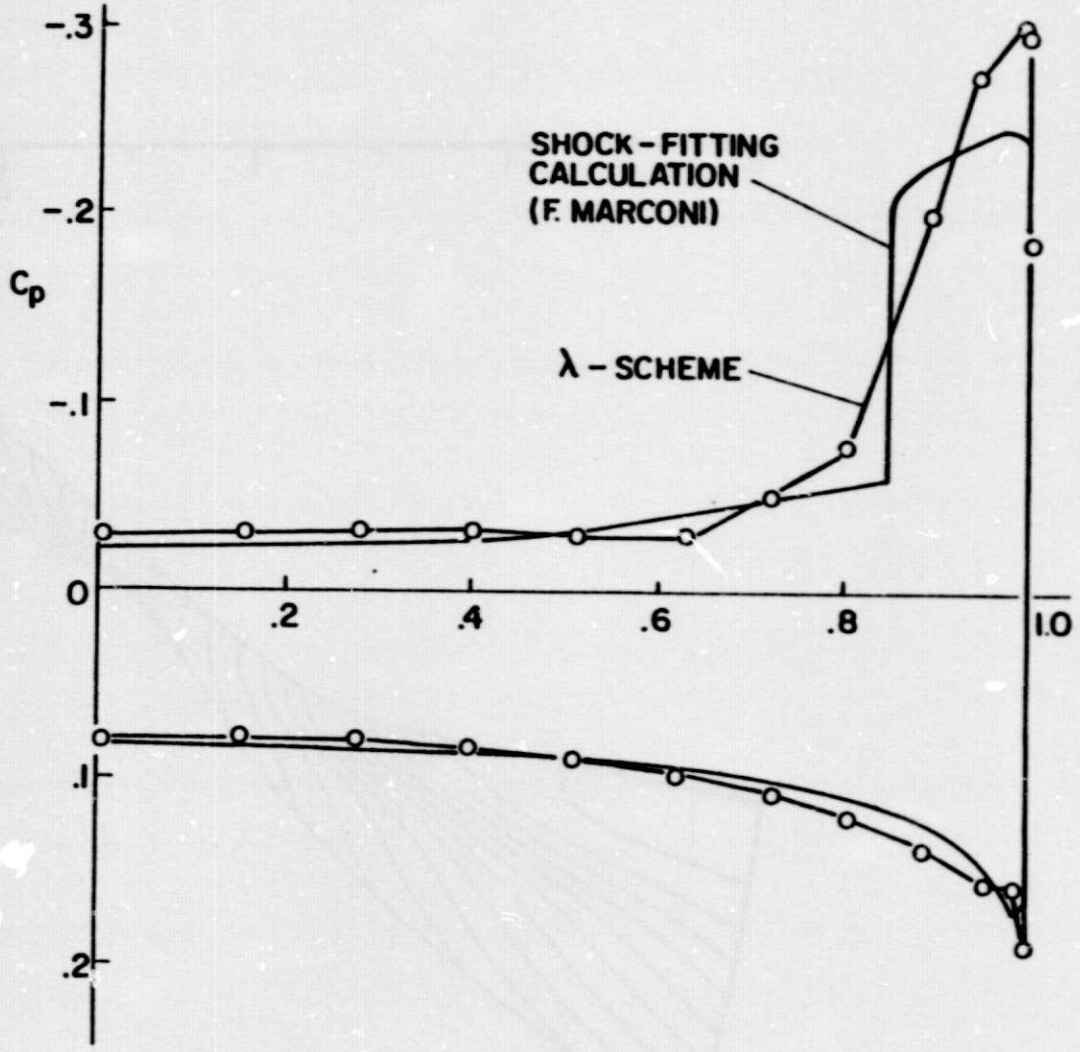

Fig. 15

Acknowledgments

The research described in the present paper was undertaken as a necessary background for a host of different applications. Some of these are sponsored by the NASA Langley Research Center, Hampton, Virginia, under Grant No. NSG 1248, and others by the Army Research Office, under Grant No. DAAG 29-77-G-0072, Project NO. P14369-E and by the Office of Naval Research, under Contract No. N00014-75-C-0511, Project No. NR 061-135.

The typing of the Report is our first attempt to a fully computerized processing of the original manuscript, which I keyed directly into a minicomputer and successively edited using a Tektronix 4006-1 terminal. The printer is a Diablo 1620-2. The success of the attempt is the result of the intelligent and dedicated labor of two undergraduate students, David Shmoys and Fred Richter, to whom I am pleased to extend a warm word of thanks.

All computational work, including the processing of the examples reported above, has been performed on a minicomputer, the PDP 11-40. Miss Catherine Fahy has prodigated her skills to assure a smooth and efficient operation of a large number of oversized programs on a machine having a maximum of 32000 addressable words and no virtual memory.